

# Laboratory experiments on the generation of internal tidal beams over steep slopes

Louis Gostiaux and Thierry Dauxois  
*Laboratoire de Physique, ENS Lyon, CNRS,  
46 Allée d'Italie, 69364 Lyon cédex 07, France*

(Dated: February 2, 2008)

We designed a simple laboratory experiment to study internal tides generation. We consider a steep continental shelf, for which the internal tide is shown to be emitted from the critical point, which is clearly amphidromic. We also discuss the dependence of the width of the emitted beam on the local curvature of topography and on viscosity. Finally we derive the form of the resulting internal tidal beam by drawing an analogy with an oscillating cylinder in a static fluid.

*Keywords:* Stratified fluids – Internal waves – Internal tides

*PACS numbers:* 47.55.Hd Stratified flows. 47.35.+i Hydrodynamic waves.

Over the past two decades it has become apparent that substantial internal tides can be generated by tidal currents over ridges and other rough topography of the ocean floor. This problem is of paramount importance since baroclinic tides, generated by barotropic currents over ocean ridges and seamounts, are an important source of the ocean interior mixing. Indeed, recent observations suggest that mixing in the abyssal oceans is rather weak, except in localized regions near rough topography. It explains the discrepancy between the observed intensity of mixing in the interior of the oceans and is required to satisfy models of ocean circulation [7]. This suggests that these topographic effects must be incorporated into realistic climate and circulation models.

This question has been studied theoretically and numerically, while related oceanic observations have been reported. Baines showed [2] first that points where the topographic slope coincides with the angle of propagation might be an effective generator of internal wave. Such a point is referred to as the critical point (see Fig. 1). Internal beams emanating from the continental slope have been observed recently [1, 9, 14, 15, 17]. On the theoretical side, let us mention several interesting descriptions [16, 18] of abrupt discontinuity cases such as a topographic step, a knife-edge ridge (zero width ridge as a simple model for tall ridges such as the Hawaiian one), a tent-shaped ridges, or smooth ridges (gaussian, polynomial). Finally, recent numerical reports have also provided some new insight about this mechanism [9, 10].

All these works converge to conclude that beams of internal tides energy arise due to the interplay between oscillating currents and bathymetric features. Of particular interest is the location where the slope is critical, i.e. where the direction of the wave beam is tangent to the slope. In the remaining of the paper, we experimentally study the location of emission and the form of the internal beam which is emitted. We also explain how this form can be predicted by drawing an analogy between the emission of an internal tide from a static topography, and the emission of internal waves by an oscillating cylinder in a static fluid. The agreement is very good, even quantitatively.

The experiment was performed in a rectangular-shaped tank (length 120 cm, height 40 cm and width 10 cm) as sketched in Fig. 1. A curved thin (0.5 cm) PVC plate, introduced before filling, played the role of the continental shelf. The experiment was performed with a linear stratification, pure water at the free surface while highly salted water at the bottom, resulting in a constant Brunt-Väisälä buoyancy frequency  $N \simeq 0.81$  rad/s. In the absence of rotation, the dispersion relation of internal gravity waves reads  $\omega = N \sin \theta$ , where  $\theta$  is the angle of the beam with respect to the horizontal.

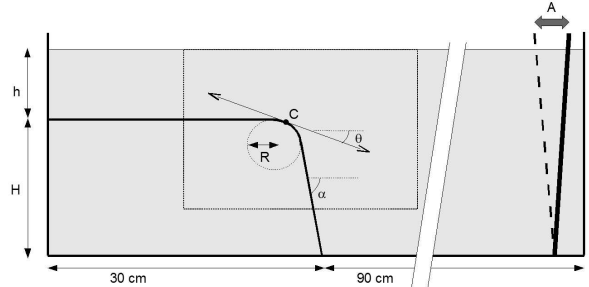


FIG. 1: Sketch of the experimental set-up. A PVC plate is oscillating between the solid and dashed oblique lines indicated on the right, creating the tide. The continental shelf consists of two planar PVC plates connected by a quarter of cylinder of radius  $R = 3.3$  cm. The upper plate is nearly horizontal, while the downgoing one makes an angle  $\alpha = 78^\circ$  with the horizontal. The aspect ratio  $h/H$  is 2/3, for a total water height  $h + H = 19$  cm. The critical point C indicates the location where the internal tide generation is supposed to occur, i.e. where the internal beam inclined at an angle  $\theta = 23^\circ$  with the horizontal is tangent to the topography. The dotted rectangle indicates the zone captured by the camera and presented in Fig. 2a.

The tidal current was generated by a second PVC plate localized far from the continental slope, i.e. in the region corresponding to the abyssal plane or to the open ocean. This plate was fixed at its bottom end, with its top end oscillating horizontally. The oscillation  $A \sin(\omega t)$  was monitored by a position control motor of a printer ap-

paratus driven by a sinusoidal electronic signal delivered by a Kepco amplifier. The phase origin at  $t = 0$  corresponds to a vertical position of the paddle and the movement is initiated leftwards towards the topography. Several forcing tidal frequencies and amplitudes were tried out. The tidal frequency  $\omega$  was satisfying the condition  $0 < \omega < N$ , so that internal tides may be freely radiating. Results and figures discussed throughout this paper correspond to  $\omega/(2\pi) = 0.050$  Hz for which  $\theta = 23^\circ$ , and  $A = 0.5$  cm.

The density gradient field within the tank was finally obtained with the standard synthetic Schlieren technique [5] by acquiring successive side views with a CMOS AVT Marlin F131B Camera. A sheet of paper with points randomly scattered was located 150 cm behind the tank. Successive images ( $1280 \times 300$  pixels) of those points obtained with the camera located 280 cm in front of the tank were adequately treated by a homemade software. A correlation image velocimetry algorithm [6] was applied between a reference image taken prior to the experiment and the different snapshots. As we used  $21 \times 21$  pixels correlation boxes with a 75% overlap, the resolution for the two dimensional density gradient field is  $256 \times 60$ .

Figure 2a show a snapshot of the vertical density gradient. To facilitate the visualization, a narrower domain than in the experiments is shown. It corresponds to the dotted rectangle depicted in Fig. 1. To increase the visibility, we filtered at the excitation frequency  $\omega$  the time series of the density gradient field over one experimental tidal period (see Ref. [12] for more details about this method).

An internal tide is clearly seen to emanate from the upper part of the slope and radiate away from the shelf-break in both directions. However, it is important to stress the absence of a third beam radiated transversally to the topography. This contradicts Baines analytical theory [2] in which this third beam reflects on the surface and is present in the general solution for the downward propagating wave. The explanation presumably lie in the presence of a singular point in Baines' case or in Saint Laurent et al numerical simulation [18]. In numerical experiments with a smooth slope and a typically shallow continental shelf [9], no such beam was found and the presence of this third beam was already ambiguous in previous experiments [3].

The amplitude of the vertical density gradient is given in terms of variations of the squared Brunt-Väisälä frequency. If one considers the original value of  $N^2 = 0.66$  rad $^2$ /s $^2$ , the measured amplitude of  $\Delta N^2 = \pm 0.005$  rad $^2$ /s $^2$  for the internal wave is a very small perturbation of the original stratification. Using the mass conservation relation

$$i\omega(\rho - \bar{\rho}) = w \frac{d\bar{\rho}}{dz}, \quad (1)$$

where  $\rho$  is the perturbed density,  $\bar{\rho}(z)$  the initial density and  $w$  the vertical density, we obtain typical vertical velocities of order  $\pm 0.11$  mm/s, corresponding to vertical

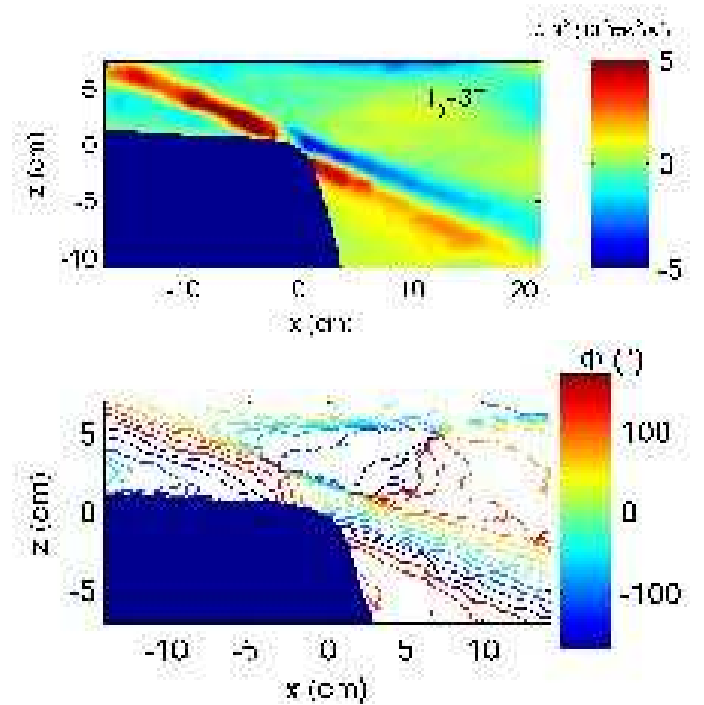


FIG. 2: (Color online) Panel a presents the two-dimensional vertical density gradient, while panel b shows the phase. Both plots have been averaged over one tidal period of the experiment around  $t = 3T$ . Horizontal and vertical distances are in cm. The generation point C appears to be an amphidromic point around which the phase of the wave rotates.

displacements of  $\pm 0.15$  mm. This is one of the interests of the synthetic Schlieren technique that allows to measure very weak perturbations of the buoyancy field and thus to investigate weakly nonlinear regimes. This vertical amplitude has to be compared to the barotropic elevation of the water induced by the forcing. The paddle oscillates with an  $A = 0.5$  cm amplitude, and the width of the free water volume in the tank is 90 cm for a height of  $H = 12$  cm. The corresponding elevation of the water at the level of the slope is thus  $\Delta H = 0.7$  mm. The baroclinic component observed is thus still a perturbation of the barotropic tide.

To the right of the generation point C, energy propagation is downward while, to the left, it is upward. As a consequence of the internal waves propagation law for which group and phase velocities are orthogonal with opposite vertical components, phase propagation is thus upward to the right and downward to the left. One can conclude from this simple observation that the phase has to rotate around C, which is therefore an amphidromic point. Our filtering technique allows to evaluate the phase of the wave [12], which is plotted in Fig. 2b. One can clearly see that the isophase lines converge on a single point previously referred as the generation point C, around which the phase rotates uniformly.

Whereas the location and the inclination of the internal tide are well understood, the selection mechanism of the width of the beam was not yet clearly identified by

previous studies. Several length scales can be considered in this problem. The first one corresponds to the thickness of the oscillating boundary layer  $\delta = (\nu/\omega)^{1/2}$  where  $\nu$  is the kinematic viscosity. In the present case,  $\delta = 1.8$  mm. The second one is the local radius of curvature of the continental shelf  $R = 3.3$  cm. At last, the dimensions of the shelf itself ( $h, H\dots$ ) that play a role [2] in the “flat-bump” geometry for which  $\alpha < \theta$  happen to be irrelevant in the configuration of a steep topography.

Our understanding is directly inspired from the generation of internal waves by oscillating cylinders. One can therefore try to draw an analogy between the internal tide generation by a curved static topography of a given radius of curvature  $R$  and the internal waves generation by an oscillating cylinder of the same radius  $R$  in a stratified fluid.

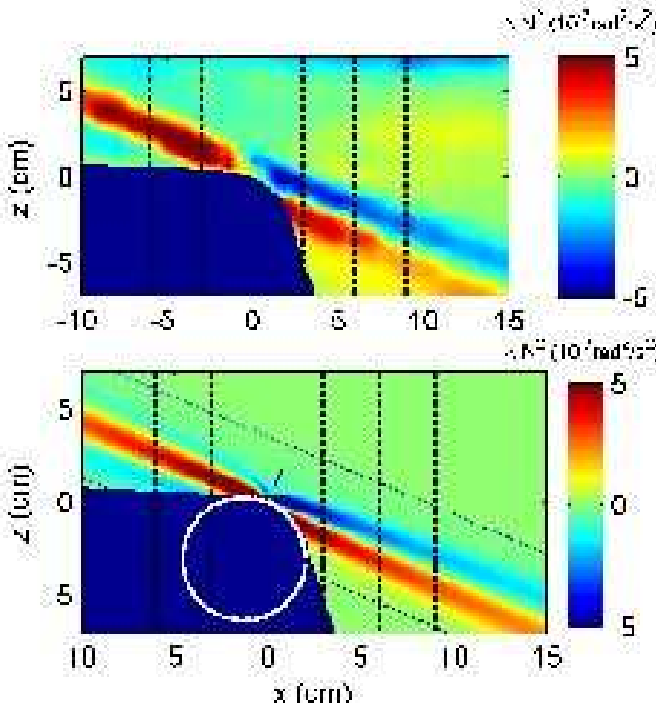


FIG. 3: (Color online) Comparison between experiment (a) and theory (b) for the vertical density gradient field. Panel (a) has been averaged over one tidal period around  $3T$ . We use the Hurley and Keady analytical solution [13] for oscillating cylinders to modelize the internal wave beam. We consider the tangential circle at the shelf break as the generating cylinder section and compute the analytical solution isolating the upper right emission point. Vertical dashed lines correspond to the cross section plotted in Fig. 4.

In their seminal theoretical work [13], Hurley and Keady showed how to get the velocity profile of the beams generated by such a cylinder. First, they proposed to consider a dimensionless parameter  $\lambda = \nu/(2R^2\omega \cot \theta)$  which is proportional to the squared ratio of the oscillatory boundary layer thickness  $\delta$  that surrounds the cylinder to its radius  $R$ . The cylinder emits the four beams of the well known St Andrew’s configuration. Each beam is considered independently. Then, the longitudinal ve-

locity component  $v_s$  for each beam is shown to be given by

$$v_s(s, \sigma) = V_0 \int_0^{+\infty} J_1(K) \exp(-\lambda s K^3/R + i\sigma K) dK, \quad (2)$$

where  $J_1$  is the Bessel function of the first kind of order 1 and  $s$  (resp.  $\sigma$ ) the longitudinal (resp. transversal) coordinate along (resp. across) the beam.  $V_0$  is the projection of the oscillation velocity along the beam. In the domain  $\delta = (\nu/\omega)^{1/2} \ll R$ , this function happens to be localized on the characteristics  $\sigma = \pm R$  corresponding to the lines of slope  $\tan \theta$ , tangential to the cylinder. In this limit case,  $2 \times 4 = 8$  beams are emitted from the four critical points of the cylinder.

In our case, we only consider the upper characteristic corresponding to the single critical point C of the problem. Hurley and Keady’s expression restricted to this single characteristic happens to fit very well our experimental data. In the tidal experiment,  $\lambda \simeq 6.3 \cdot 10^{-4}$ . We estimate the buoyancy perturbation of the stratification by means of Eq. (1). By appropriately taking into account the inclination of the beam, one gets a final expression for the vertical density gradient that can be compared to our experimental data.

Fig. 3 compares the vertical density gradient field in the experimental (a) and the theoretical (b) cases. The analytical solution of Hurley and Keady is computed on an imaginary cylinder tangential to the shelf break region. The amplitude of oscillation of the cylinder corresponds to the amplitude of the tidal flow. The agreement is qualitatively very good. The phase opposition between the two parts of the beams is also well described by the model.

To get a more quantitative comparison between experiment and theory, we plot on Fig. 4 five vertical cross sections (indicated in Fig. 3) of the vertical density gradient field at  $x = -6, -3, 6$  and  $9$  cm relative to the generation point. The quantitative agreement between the experimental and the theoretical profiles is very good, which confirms that the structure of the emitted beam only depends on the viscous boundary layer thickness  $\delta$  and on the local radius of curvature of the shelf  $R$ .

First of all, this experiment proves that the internal tide generation conditions are met when the radiated tidal beam is aligned with the slope of the topography, corresponding to a critical point of emission which happens to be amphidromic. We clearly demonstrate the absence of any transverse emission at that point that is supposed to occur in Baines analytical study [2]. It is however important to emphasize that this disagreement might come from the absence of any sharp corner in the shelf break, contrary to what has been considered in Refs [2, 3, 18]. Following this observation, we derive a simple analytical model derived from the theoretical work of Hurley and Keady [13] and show that we can quantitatively estimate the density perturbation profile as a function of the viscosity and the local radius of cur-

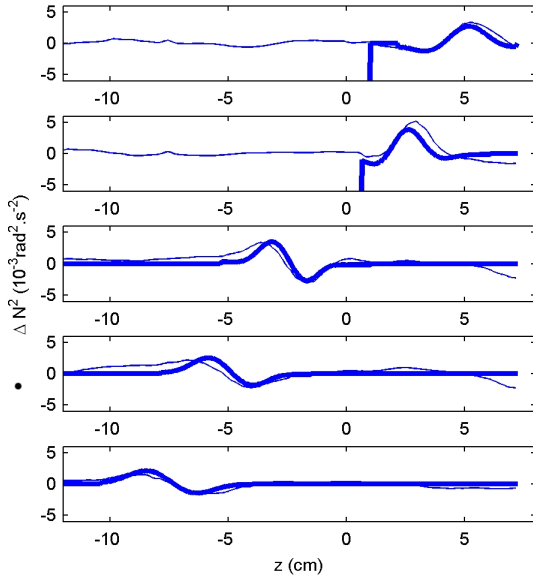


FIG. 4: Vertical cross sections of the measured vertical density gradient (thin line) and its theoretical prediction using Hurley and Keady's theory (bold line). From top to bottom, the cross sections correspond to the abscisse  $x = -6, -3, 3, 6$  and  $9$  cm.

---

[1] A. Azevedo, J. C. B. da Silva and A. L. New. *On the generation and propagation of internal solitary waves in the southern Bay of Biscay*. *Deep-Sea Research I* 53: 927-941 (2006).

[2] P. G. Baines. On the internal tide generation models. *Deep-Sea Research* 29:307-338 (1982).

[3] P. G. Baines and F. Xin-Hua, Internal tide generation at a continental shelf/slope junction: a comparison between theory and a laboratory experiment. *Dynamics of Atmospheres and Oceans* — 9:297 (1985).

[4] S. Cardoso and J. C. B. Da Silva. Generation sites of internal waves observed by ERS SAR off the SW coast of Portugal. Interesting results concerning ray reflection. XVII International Conference for Physics Students, Budapest, Hungria (2002).

[5] S. B. Dalziel, G. O. Hughes and B. R. Sutherland. Whole density field measurements by synthetic schlieren. *Experiments in Fluids* 28:322 (2000).

[6] A. Fincham and G. Delerce. Advanced optimization of correlation imaging velocimetry algorithms. *Experiments in Fluids*, 29:13, 2000.

[7] C. Garrett. *The dynamic ocean in Perspectives in Fluid Dynamics*, G. K. Batchelor, H. K. Moffatt, and M. G. Worster (Eds.) Cambridge University Press, 2005.

[8] T. Gerkema. Internal and interfacial tides: beam scattering and local generation of solitary waves. *Journal of Marine Research* 59:227-255 (2001).

[9] T. Gerkema, F.-P. A. Lam and L. R. M. Maas. Internal tides in the Bay of Biscay: conversion rates and seasonal effects. *Deep-Sea Research II* 51:2995-3008 (2004).

[10] T. Gerkema, C. Staquet and P. Bouruet-Aubertot. Decay of semi-diurnal internal tide beams due to subharmonic resonance. *Geophysical Research Letters* 33, L08604 (2006).

[11] L. Gostiaux, PhD Thesis, ENS Lyon (2006). Étude expérimentale des ondes internes: génération, propagation et réflexion.

[12] L. Gostiaux, T. Dauxois, H. Didelle, J. Sommeria and S. Viboux. Quantitative laboratory observations of internal wave reflection on ascending slopes. *Physics of Fluids* 18, 056602 (2006).

[13] D. G. Hurley and G. Keady. The generation of internal waves by vibrating elliptic cylinders. Part 2. Approximate viscous solution. *Journal of Fluid Mechanics* 351, 119-138 (1997).

[14] N. Jézéquel, R. Mazé and A. Pichon. Interaction of semidiurnal tide with a continental slope in a continuously stratified ocean. *Deep-Sea Research I* 49:707-734 (2002).

[15] A. L. New and R. D. Pingree. Local generation of internal soliton packets in the central Bay of Biscay. *Deep-Sea Research* 39:1521-1534 (1992).

[16] F. Petrelis, S. Llewellyn Smith and W. R. Young, Tidal conversion at a submarine ridge. *Journal of Physical Oceanography* 36: 1053-1071 (2006).

[17] R. D. Pingree and A. L. New, Abyssal penetration and bottom reflection of internal tidal energy in the bay of biscay. *Journal of Physical Oceanography* 21:28-39 (1991)

[18] L. St. Laurent, S. Stringer, C. Garrett and D. Perrault-Joncas. The generation of internal tides at abrupt topography. *Deep-Sea Research I* 50:987 (2003).

ture of the topography.

Since this paper focuses on the internal tide generation, we do not consider the evolution of the internal tides as they propagate further into the deep ocean. Surface reflections, in particular, are expected to generate internal solitary waves by creating local disturbances at the seasonal thermocline [8, 15].

Moreover, the emitted internal wave of tidal period often breaks up into internal waves of shorter period. Indeed, and very interestingly, a recent numerical report has emphasized that parametric subharmonic resonance may come into play in the rotating case [10]. Experimental work along those lines is in progress.

## Acknowledgments

We thank F. Petrelis and S. Llewellyn Smith for helpful discussions. Comments to the manuscript by Denis Martinand are deeply appreciated. This work has been partially supported by the 2005 PATOM CNRS program and by 2005-ANR project TOPOGI-3D.